Structural Differences Exhibited by Networks Prepared by Chemical and Photochemical Reactions. III. Characterization by Inverse GPC

B. HAIDAR, A. VIDAL, H. BALARD, and J. B. DONNET, *Centre de Recherches sur la Physico-Chimie des Surfaces Solides, C.N.R.S., F-68200 Mulhouse, France*

Synopsis

The use of a new method, inverse GPC, as a tool for the characterization of elastomeric networks, allowed the obtaining of the distribution curves of the network strands. In agreement with previous studies it was shown that photocrosslinked materials exhibit a more homogeneous distribution of the crosslink points than do peroxide cured samples. From the GPC distribution curves, it was possible to calculate $\bar{M}_c$, the average molecular weight of a network strand.

INTRODUCTION

In previous papers[1-4] we reported experiments related to the photocrosslinking processes occuring in elastomeric films (EPDM) containing benzoin derivatives as photosensitive initiators. The resulting networks which were compared to peroxide-cured EPDM were characterized through their stress–strain and thermoelastic properties and by measurement of their swelling ratio (V_{2m}). The results obtained suggested, on the one hand, that photocrosslinked materials exhibit a more homogeneous distribution of the crosslinks than do peroxide cured elastomers and, on the other hand, that the homogeneity of the photocrosslinked materials is dependent on the photosensitive system used.

In order to confirm these results, we tried to characterize our samples by a method unrelated to the theories of elasticity. We anticipated that inverse GPC could provide the needed information.

Gel permeation chromatography is useful for the determination of the molecular weight of a solute. However, when the size of the latter is known, it can be used to characterize the gel constituting of the stationary phase (determination of its pore sizes and distributions). Then it will be referred to as inverse GPC. The porosity of rigid particles is usually determined either through gas adsorption (BET method) or mercury porosimetry.[5-7] Comparison of pore size measured by the latter techniques with the molecular weight of macromolecules eluted on the same adsorbents allowed Halasz and colleagues[8,9] to establish a linear relationship between both parameters.

Inverse GPC can thus be used for the characterization of solids as long as the corresponding materials can behave as stationary phase and do not exchange any specific interactions with the selected probe. The applicability

Journal of Applied Polymer Science, Vol. 29, 4309–4320 (1984)
 CCC 0021-8995/84/124309-12$04.00

of the method has been checked with a large number of stationary phases such as silica gels, glass fibers, aluminum or tungsten oxide,[8,10,11] and even swollen gels of polystyrene.[12] However, to our knowledge this method has not been applied to highly crosslinked rubber networks ($V_{2m} < 0.5$), and we anticipated that it could provide an original way of characterizing the topology and size distribution of the network strands.

The use of rubber networks for this particular application implied the following

—the adjustment of the method using standard adsorbants such as silica (with well characterized porosity);

—the preparation of chromatography columns, exhibiting a good separating power, filled with elastomeric networks;

—the determination, from the obtained results, of the degree of crosslinking of the networks, and the comparison of the corresponding values with those provided by mechanical properties or swelling ratio measurements.

EXPERIMENTAL

Materials and General Procedures

The polymer selected for study was a terpolymer EPDM Nordel 1440, obtained from E.I. DuPont de Nemours: poly(ethylene-co-propylene-co-1,4 hexadiene).

The equipment used to perform the UV irradiations (254 nm) as well as the processes selected to characterize the crosslinked materials (IR spectroscopy, swelling in cyclohexane, . . .) were described previously.[1-4]

All chemicals were reagent grade and purified by standard procedures. The curing of the elastomer with variable amounts of dicumyl peroxide resulted from heating it at 160°C under 25×10^6 Pa for 2 h. The chemical bonding of the chromophore (benzene ring) on the EPDM backbone was performed by means of Friedel–Crafts reactions and was described previously.[2-4]

Prior to any measurement all networks were submitted, at room temperature, to a prolonged extraction with cyclohexane in order to eliminate uncrosslinked rubber. The amount of soluble material removed was used to calculate the fraction of initial elastomer successfully introduced in the network.[3] For the samples used in the present paper this fraction was always higher than 90%.

GPC Apparatus

The solvent used for GPC was freshly distilled THF stored under nitrogen. The high pressure pump was a Spectra Physics 740B. The loop of the injection valve (Valco) had a capacity of 50 μL, and the detection was performed by use of an Optilab differential refractometer (cell path length = 10 mm).

The columns and the refractometer were placed in a thermostated enclosure (24°C). The stationary phases were either crosslinked EPDM or standard silicas for use as reference and for the adjustment of the method.

Preparation of the Columns

Crosslinked EPDM. We used Gilson glass columns, 1 m long, 0.6 cm in diameter. They were packed with polymer pieces obtained by mechanically grinding plates or films of the crosslinked elastomer. In order to obtain gel pieces of small size and narrow distribution, we went through the following steps:

1. selection of well characterized photocrosslinked or peroxide cured elastomers;
2. mechanical grinding of the samples for 2–3 h;
3. sifting on a series of sieves (mesh size in the range 500–100 μm);
4. ultrasonic dispersion of the sieved samples in ethanol (destruction of aggregates);
5. a narrow size distribution of the particles was attained by elutriation in methanol;
6. washing followed by ultrasonic dispersion of the selected particles in the solvent used for GPC (THF);
7. homogeneous packing of the columns according to the method developed by Heitz et al.[13]

Porous Silicas. Three silicas were selected: Spherosil XOA 600 (600 m^2/g; Rhône-Poulenc); Spherosil XOA 800 (800 m^2/g; Rhône-Poulenc); Spherosil B 980 (380 m^2/g; Rhône-Poulenc).

They had an average aggregate diameter equal to 5 μm. Their porosity was controlled by nitrogen adsorption (Micromeritics, Mod. 2100D). BET[14] and BJH[15] methods were applied to determine respectively their specific surface area and pore size distribution. The columns (30 cm long, 4 cm in diameter) were packed according to the method developed by Bar et al.[16]

Measurements

Polystyrenes of various molecular weight were generally used as probe (Polymer Standards Chrompack: 510, 2000, 8000, 32,000, 232,000 g mol^{-1}). However, other compounds were also checked: polyethylene oxide (Merck, 200, 400, 600 g mol^{-1}); polypropylene oxide (Fluka, 400, 1200, 2000 g mol^{-1}); alkanes (Merck, C_5–C_{35}).

A 1% solution of each compound in THF was injected, the solvent flow rate being set at 0.4 cm^3 mn^{-1}. When using EPDM as stationary phase, the pressure at the outlet of the column was moderate (6×10^5 Pa) while it was much higher with silica (30×10^5 Pa).

RESULTS AND DISCUSSION

In order to test the validity of inverse GPC as a tool for the characterization of a stationary phase, the method was adjusted by use of porous silicas.[8] Then it was extended to the characterization of rubber networks.

Inverse GPC on Porous Silicas

The selected silicas were carefully characterized, particularly on the point of view of their pore size distribution.

Determination of the Silica Porosity by Gas Adsorption. The porosity

of the selected silicas (Spherosil XOA 600, Spherosil XOA 800, and Spherosil B 980) was measured by gas adsorption. The cumulative and distribution curves of Spherosil XOA 600 and XOA 800 pore size are presented in Figures 1 and 2. It appears that:

—XOA 800 exhibits a narrower pore size distribution than XOA 600;

—the radius of the main pore family (maximum of the distribution curve) of XOA 800 is smaller (6 Å) than that of XOA 600 (9 Å);

—the ratio associated with this family is greater in XOA 800 (26%) than in XOA 600 (14%).

After characterizing their porosity, the behavior of these silicas as stationary phase in GPC was checked.

Inverse GPC on Silica. Solutions of polystyrene of well-known molecular weight have been eluted on the silica columns. It is possible to relate the molecular weight of each eluted molecule to the fraction of the column to which it is accessible. This fraction of available volume is given by

$$K_{av} = \frac{V_e - V_0}{V_t - V_0}$$

in which V_0 and V_t are respectively the outer and total volume of the column and V_e is the elution volume of a probe whose molecular weight is M.

Conversely $(1 - K_{av})$ is the volume fraction of the column unavailable to a molecule of a given size. Plotting $(1 - K_{av})$ vs. log M yields the cumulative curves of the eluted masses from which the corresponding distribution curves can be derived (Figs. 3 and 4). It appears from Figure 4 that:

—the distribution of the eluted masses is narrower on XOA 800 than on XOA 600;

—the mass associated with the maximum of the distribution curves is smaller on XOA 800 (log M = 2.95 vs. 3.25 on XOA 600);

—the ratio associated with this family is greater on XOA 800 (19% vs. 8% on XOA 600).

If a pore of a given size can be associated with a given eluted mass, the distribution curves of eluted masses and pore size could then be assumed to be identical.

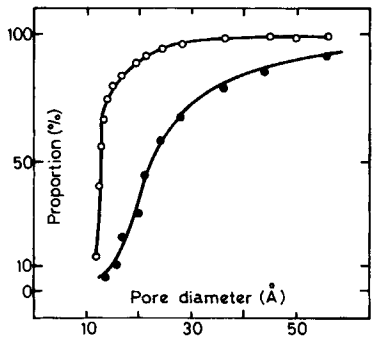

Fig. 1. Cumulative curves of pore diameter: (○) XOA 800; (●) XOA 600.

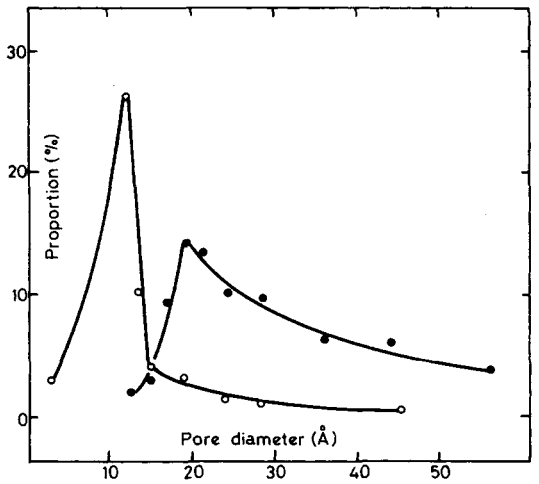

Fig. 2. Distribution curves of pore diameter: (○) XOA 800; (●) XOA 00.

Comparison of Results Yielded by GPC and Gas Adsorption. Comparison of Figures 2 and 4 points to a good agreement between both techniques, particularly on the point of view of the shape of the curves as well as the relative position of the maxima.

These results tend to show that the molecular weight of each eluted oligomer is associated with a pore of a given size.

For each silica the discrepancies between the ratios at the maxima of the distribution curves obtained by BJH or GPC could be the result of differences in the size of the probes used (N_2 vs. polystyrene oligomers).

We tried to determine the equation of a calibration curve linking the molecular weight of an eluted molecule to the size of the corresponding pore. Since the most precise points of the distribution curves are those corresponding to the maxima, these values were particularly used. In order to increase the number of experimental points, we also plotted the GPC distribution curves of other silicas whose characterization by BJH is reported in the literature.[17] These silicas were Sperosil XOA 200 (125–250

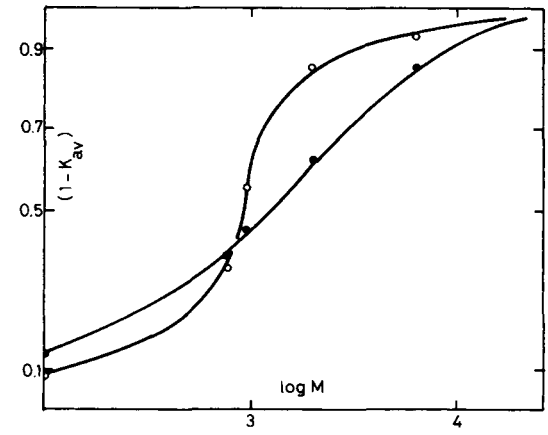

Fig. 3. Cumulative curves of eluted masses: (○) XOA 800; (●) XOA 600.

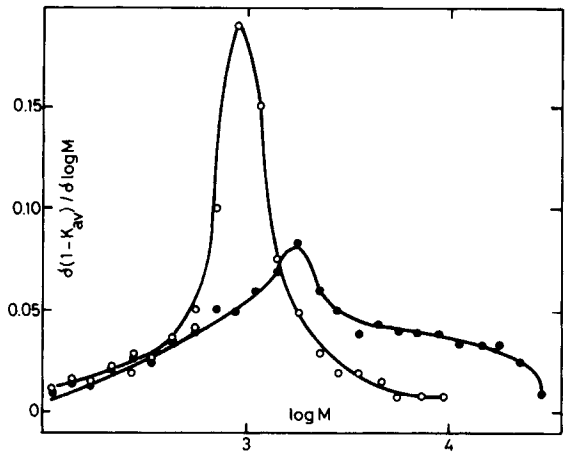

Fig. 4. Distribution curves of eluted masses: (○) XOA 800; (●) XOA 600.

m^2/g; Rhône-Poulenc), Spherosil XOB 075 (50–100 m^2/g; Rhône-Poulenc), and Spherosil XOB 030 (25–40 m^2/g; Rhône-Poulenc). The results obtained are reported in Table I.

By plotting log R_{max} vs. log M_{max} a linear relationship is obtained. The equation of this curve determined by least square analysis is (determination coefficient, $R^2 = 0.995$):

$$\log M = 1.3 + 1.54 \log R \tag{1}$$

This equation is that of a calibration curve linking the radius R of the smallest pore available to a molecule of polystyrene dissolved in THF to its molecular weight. This equation is in satisfactory agreement with the theoretical relationships established by Van Kreveld and Van Den Hoed[18] or Halasz and Colleagues,[8,9,19] which are respectively log $M = 1.5 + 1.7$ log R and log $M = 0.86 + 1.7$ log R.

The validity of the method having been checked, it was extended to the characterization of rubber networks.

Inverse GPC on EPDM Networks

The GPC columns packed with pieces of crosslinked Nordel were prepared according to the process described in Experimental. We checked that the elaborate sample preparation procedure followed for the packing of the

TABLE I
Characterization of Several Silicas by BJH and GPC

Silica	R_{max} (Å) BJH	log M_{max} GPC	Ref.
Spherosil XOA 800	6	2.95	—
Spherosil XOA 600	9	3.25	—
Spherosil B 980	32	3.55	—
Spherosil XOA 200	100	4.45	16
Spherosil XOB 075	125	4.65	16
Spherosil XOB 030	375	5.15	16

columns did not alter the network structure. It was particularly shown that a prolonged ultrasonic treatment (several hours) did not induce any change in the $M_{cV_{2m}}$ value of a given sample (because swelling measurements are difficult to perform on powders, this verification was conducted on an unground sample). As for the mechanical grinding, if it could be associated with an evolution of the surface layer of the polymer particles, no modification of the bulk of the elastomer was expected (as a matter of fact, the good agreement of the results yielded by GPC with those obtained by swelling supports such an assumption). Similarly it was shown by chemical relaxation[20] that, in the particular range of temperature used for the experiments, peroxide-cured and photocrosslinked materials do not exhibit any difference in the lability of their crosslinks. We were thus able to assume that the networks used for column packing were representative of their original crosslinked structure.

Two couples of columns were used, each one constituted by peroxide-cured Nordel and photocrosslinked EPDM. We took care to use samples having the same crosslinking degree determined by swelling. Table II provides the main features of the columns.

It appears that they exhibit satisfactory characteristics. Use of networks of smaller crosslinking degrees should have been of interest. However, since lightly crosslinked materials were unable to sustain the pressure, it was impossible to prepare any column of this kind.

The elution of THF solutions of polystyrene oligomers on columns A_1 and B_1 provided the chromatograms reported in Figure 5. It appears that B_1 has a better separating power than A_1. Since both columns are made out of the same elastomer and have the same crosslinking degree (determined by swelling in cyclohexane) such a difference can only be attributed to a discrepancy in the distribution of the size of the network strands.

Similarly to what was done with silica, different probes were used (solutions of polystyrenes of well-known molecular weight in THF). The cumulative curves of the eluted masses obtained by plotting $(1 - K_{av})$ vs. log $\overline{M}$ are reported in Figure 6. One notes that the separation domain of column A_1 corresponds to a much larger range of molecular weights than does B_1. Conversely, the latter is more efficient in a narrower range of eluted masses. Derivatization of curves of Figure 6 yields the distribution curves of eluted masses (Fig. 7). Thus B_1 exhibits a much narrower distribution curve than A_1.

In agreement with what was done with silicas (the mass of each eluted

TABLE II
Characteristics of the Columns

Columns	$\overline{M}_{cV_{2m}}$[a] (g mol^{-1})	V_0 (cm^3)	V_t (cm^3)	Plate count	Pressure at 0.4 mL/mn (Pa $\times$ 10^{-5})
A-1 Peroxide	4000	15.0	35	3000	5.9
B-1 Photocross	4000	14.6	36	3500	4.9
A-2 Peroxide	2000	17.0	36	1800	6.9
B-2 Photocross	2000	18.6	34.5	2600	5.9

[a] Average molecular weight of a network strand deduced from swelling ratios.

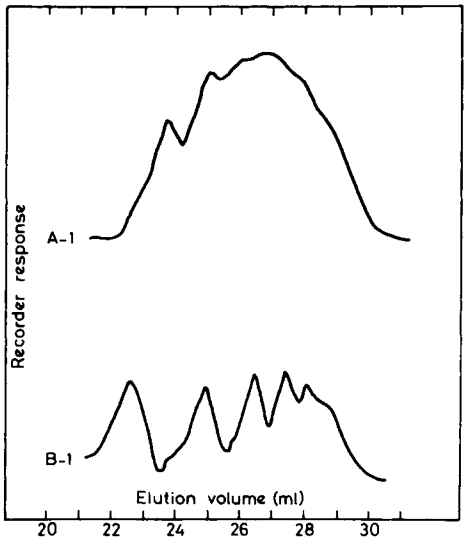

Fig. 5. Chromatograms of polystyrene oligomers.

molecule corresponds to an available volume in the network), the distribution curves of the eluted masses were identified with the distribution curves of the size of the network strands. The latter is therefore narrower for B_1 than for A_1.

It is worth noticing that the maxima of the distribution curve of both samples correspond to the same molecular weight ($\log \overline{M} = 2.55$). This is in agreement with the fact that A_1 and B_1 have the same crosslinking degree determined by swelling. By use of the calibration curve plotted with silicas, the radius of the volume accessible to the molecule whose mass corresponds to the maximum of the distribution curves is close to 5.6 Å.

Then we investigated the possibility of establishing a relationship between the crosslinking degree of the network and its available volume.

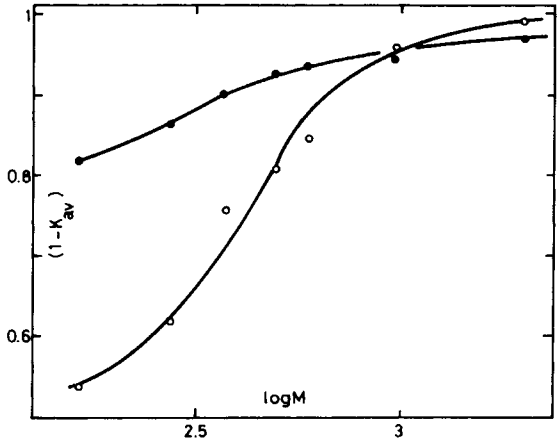

Fig. 6. Cumulative curves of eluted masses: (●) A-1; (○) B-1.

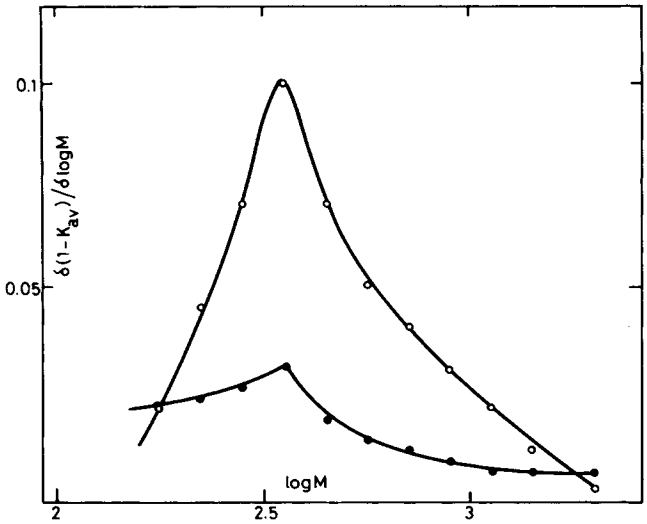

Fig. 7. Distribution curves of eluted masses: (●) A-1; (○) B-1.

Determination of $\overline{M}_c$ from GPC Results

It is known that in a tetrafunctional network each crosslink A is bound to four topological neighbors (Fig. 8) through chains whose molecular weight is $\overline{M}_c$.[21] Moreover, this same point, A, will also be surrounded by spatial neighbors S to which it is unrelated. If the distance AT determines the extensibility of the strained network, AS will determine the size of a molecule percolating through the network. AS is, of course, related to the crosslinking degree, i.e., to $\overline{M}_c$. As shown by Flory,[22] in a dry amorphous state, the volume of voids in a polymer is negligible. As a consequence, a dried network is totally impenetrable even to the smallest molecule. This behavior is, of course, completely different when considering a swollen network. In this case, indeed, accessible voids will be available between network strands.

For a dried network whose density and critical molecular weight are, respectively, ρ and $\overline{M}_c$, the number of chains per unit volume is given by

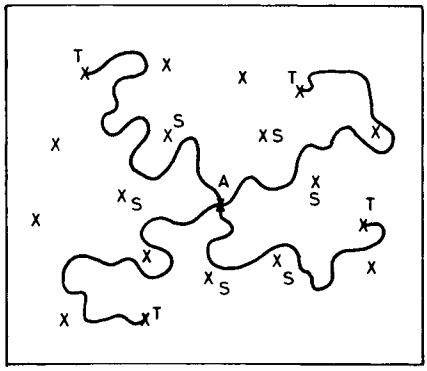

Fig. 8. Structure of a tetrafunctional elastomeric network.

$$\nu = \rho/\overline{M}_c$$

As a consequence, the number of crosslinks per unit volume will be

$$n = \frac{N\rho}{2\overline{M}_c \times 10^{24}}, \quad N = \text{Avogadro's number}$$

Therefore, the average volume available for each crosslink can be expressed as

$$\frac{1}{n} = V_p = \frac{2\overline{M}_c \times 10^{24}}{\rho N}$$

If this volume is compared to a sphere, its radius will be

$$r = \left[\frac{3}{4\pi}\frac{2\overline{M}_c \times 10^{24}}{\rho N}\right]^{1/3}$$

which is in agreement with that of Rempp and Hertz.[23] This radius is, of course, equal to half the distance separating A from its closest spatial neighbor (S). It was previously shown[22] that in the dry state this volume $4\pi r^3/3$ is totally occupied by the network chains. If V_{2m} is the volume fraction of the network in the swollen state, the corresponding radius will be

$$r_s = rV_{2m}^{-1/3}$$

After swelling an accessible volume will be liberated, assimilated to a sphere, its radius will be

$$R = r_s - r = r(V_{2m}^{-1/3} - 1) = \left[\frac{3}{4\pi}\frac{2\overline{M}_c \times 10^{24}}{\rho N}\right]^{1/3}(V_{2m}^{-1/3} - 1)$$

i.e.,

$$\overline{M}_c = \left[\frac{R}{(V_{2m}^{1/3} - 1)}\right]^3 0.4\pi\rho \qquad (2)$$

For a given swelling ratio the latter relationship will provide a way to determine $\overline{M}_c$ from the R value yielded by inverse GPC. Determination by this process of the crosslinking degree of the networks used as inverse GPC stationary phase gave the results reported in Table III.

The results obtained are in fairly good agreement with those yielded by swelling. As a consequence, if each eluted mass can be associated with a given available volume and therefore with a particular $\overline{M}_c$, the distribution

TABLE III
Comparison of the Average Molecular Weight of Network Strands Deduced from GPC and Swelling Ratios

Sample	log $\overline{M}$[a]	R (Å)[b]	$\overline{M}_c$[c]	$\overline{M}_{cV_{2m}}$[d]
A-1	2.55	6.5	4600	4000
B-1	2.55	6.5	4600	4000
A-2	2.54	5.6	2500	2000
B-2	2.54	5.6	2500	2000

[a] Mass corresponding to the maximum of the GPC distribution curves.
[b] Radius of the accessible volume deduced from relation (1).
[c] Average molecular weight of a network strand deduced from GPC relation (2).
[d] Average molecular weight of a network strand deduced from swelling ratios.

curves of the eluted masses are identical to that of the network strands. The results obtained are thus in agreement with the results yielded by the study of mechanical properties. Moreover, it is worth noticing that the decrease of the radius of the available volume with an increase of the crosslinking degree of the network is in agreement with observations due to Brun et al. when characterizing crosslinked resins by thermoporometry.[24]

CONCLUSION

A new method, inverse GPC, has been developed for the characterization of rubber networks. Independent of the different theories of elasticity, this method provides an access to the distribution of the length of the network strands. It particularly shows, in agreement with previous studies, that their distribution is much narrower when the networks are obtained by photocrosslinking process than when they are the result of peroxide curing. This effect is particularly enhanced when the chromophore is grafted on the polymer backbone.

Further work will consider the effect of the crosslinking process used on the structure of the resulting network, particularly on the point of view of the nature of the created bonds.

References

1. J. A. Bousquet, J. B. Donnet, J. Faure, J. P. Fouassier, B. Haidar, and A. Vidal, *J. Polym. Sci., Polym. Chem. Ed.*, **17**(6), 1685 (1979).
2. J. A. Bousquet, J. B. Donnet, J. Faure, J. P. Fouassier, B. Haidar, and A. Vidal, *J. Polym. Sci., Polym. Chem. Ed.*, **18**(3), 765 (1980).
3. B. Haidar, A. Vidal, and J. B. Donnet, *Br. Polym. J.*, **14**(9), 126 (1982).
4. B. Haidar, A. Vidal, and J. B. Donnet, *Br. Polym. J.*, **15**(6), 120 (1983).
5. C. Pierce, *J. Phys. Chem.*, **57**, 149 (1953).
6. S. J. Gregg and K. S. W. Sing, in *Adsorption, Surface Area and Porosity*, Academic, New York, 1967, p. 162.
7. H. L. Ritter and L. C. Drake, *Ind. Eng. Chem. Anal. Ed.*, **17**, 782 (1945).
8. I. Halasz and K. Martin, *Angew. Chem. Int. Ed. Engl.* **17**, 901 (1978).
9. W. Werner and I. Halasz, *J. Chromatogr. Sci.*, **18**, 277 (1980).
10. L. F. Martin, F. B. Blouin, and S. P. Prowland, in *Gel Permeation Chromatography*, K. H. Altgelt and L. Segal Eds., Marcel Dekker, New York, 1971.
11. K. Martin, PhD thesis, Saarbrücken, 1975.
12. D. H. Freeman and I. C. Poinescu, *Anal. Chem.*, **49**(8), 1183 (1977).
13. W. Heitz and J. Coupek, *J. Chromatogr.*, **36**, 290 (1968).

14. S. Brunauer, P. H. Emmet, and E. Teller, *J. Chem. Soc.*, **60**, 309 (1938).
15. E. Barrett, L. Joyner, and P. Halenda, *J. Am. Chem. Soc.*, **73**, 377 (1951).
16. D. Bar, M. Caude, and R. Rosset, *Analusis*, **4**(3), 108 (1976).
17. Z. Gallot, PhD thesis, Strasbourg, 1970.
18. M. E. Van Kreveld and N. Van Den Hoed, *J. Chromatogr.*, **83**, 111 (1973).
19. R. Nicolov, W. Werner, and I. Halasz, *J. Chromatogr. Sci.*, **18**, 207 (1980).
20. B. Haidar, A. Vidal, and J. B. Donnet, to appear.
21. P. J. Flory, *Proc. Roy. Soc. London*, **A351**, 351 (1976).
22. P. J. Flory, *Rubber Chem. Tech.*, **48**, 513 (1975).
23. P. Rempp and J. Hertz, *Angew. Makromol. Chem.*, **76/77**(1126), 373 (1979).
24. M. Brun, J. F. Quinson, R. Blanc, M. Negre, R. Spitz, and M. Bartholin, *Makromol. Chem.*, **182**, 873 (1981).

Received January 3, 1984
Accepted April 18, 1984